

Strengthen strategies for reinforced concrete haunched beams using fibre reinforced polymer fabric and engineered cementitious composites

Farqad Qays Ibrahim

Civil Engineering Department, Gaziantep University, Gaziantep, Turkey
University of Technology, Baghdad, Iraq

ABSTRACT

External strengthening of reinforced concrete haunched beams with and without shear reinforcement has been investigated by using carbon and basalt fiber reinforced polymer fabrics. In addition, the flexural behavior of reinforced haunched beams which are partially and entirely produced from engineered cementitious composite has been tested. The samples, which were produced from self-compacting concrete, engineered cementitious composite, and a combination of them, were prepared and tested via four-point loading tests. Reinforced haunched beams were divided into two strengthening groups. Group 1 included the shear strengthening of self-compacting concrete reinforced haunched beams (beams without stirrups) by the consideration of various strengthening configurations with both fiber-reinforced polymer fabric types. Group 2 included the flexural strengthening of reinforced haunched beams via fiber-reinforced polymer fabrics and/or engineered cementitious composite. The obtained results were depended on the ultimate load capacities, load-displacement curves, crack patterns, and failure modes of strengthened reinforced concrete haunched beams. Experimental results show that the strengthening material and strengthening configuration influence the mechanical behavior of reinforced concrete haunched beams considerably. However, the effect of strengthening configuration was higher. The highest increase in load capacity was 72.8% for shear strengthening (group 1), while the highest increase was 28.8% for the flexural strengthening group (group 2). Furthermore, the U-shaped anchorage with fiber-reinforced polymer fabrics prevented the premature failure of engineered cementitious composite layer and fiber-reinforced polymer fabrics covering the bottom face of reinforced haunched beams and increased the load capacity of reinforced haunched beams, while some losses were observed in ductility. The replacement of the concrete with engineered cementitious composite on the tension side increased the load capacity of reinforced concrete haunched beams.

Abbreviation:- RCHB: reinforced concrete haunched beam, CFRP: carbon fiber reinforced polymer, BFRP: basalt fiber reinforced polymer, RHB: reinforced haunched beam, ECC: engineered cementitious composite, SCC: self-compacting concrete, FRP: fiber reinforced polymer, RC: reinforced concrete, EB-FRP: externally bonded fiber-reinforced polymers, GFRP: glass fiber reinforced polymer, HRWRA: high range water reducing admixture called (Sika ViscoCrete), PVA: poly vinyl alcohol, SCCHB: self-compacting concrete haunched beams, LVDT: linear variable displacement transducer, FF: Flexural failure, SF: Shear failure.

Keywords: Shear strengthening; Flexural strengthening; Composites Fabrics; U-jacket strips anchorage; Cracking patterns.

Corresponding Author:

Farqad Qays Ibrahim
University of Technology
Baghdad, Iraq
farqadqays20@gmail.com

1. Introduction

Over the years, fiber-reinforced polymer fabric has continued to show one of several great encouraged and economical engineering solutions for strengthening reinforced concrete (RC) structures. FRP materials are an

outstanding option as an external strengthening technique due to their lightweight, corrosion resistance, and high strength. The externally bonded fiber-reinforced polymers (EB-FRP) represent one of the most popular and preferable strengthen techniques for engineers due to ease of installation, lower cost, and preventing chloride ions from penetrating concrete [1, 2]. Flexural (FF) and shear failure (SF) are the major modes of failure in RC beams. FF is commonly favored to the SF, as the previous is ductile; however, the SF is brittle. A stress redistribution and warning to occupants are the most preferable characteristic provided by the ductile failure; however, a brittle failure is sudden and thus disastrous. Strengthening is required to make a shear or flexure-deficient RC beam sufficiently strong. Several types of research have been investigated for the potential use of CFRP for both flexural [1 - 7] and shear strengthening of concrete beams [8 - 10]. Side bonding, U-jacketing, and complete wrapping are the most common FRP strengthening techniques [11]. The effect of the U-jacketing method on RC beams performance has been investigated for both flexural [1], [12- 15] and shear behavior [12], [16 - 19]. By comparing BFRP to GFRP reinforcement, it exhibits higher tensile strength (f_{ct}), and similar tensile modulus [20], the use of BFRP is an effective way to repair and strengthen weakened structures [21]. SCC as a high-performance concrete with enhanced rheological behavior can flow around reinforcing bars or other obstacles while resisting dynamic segregation and maintaining its homogeneity, and efficiently fill even highly congested or complex formwork, to fully encapsulate the reinforcement, purely under its weight and without the need of mechanical vibration, and produce a dense and stable, high-quality end product [22]. Because of its great improvement in the quality of concrete structures, many studies have been conducted on the SCC, which has opened up new areas for concrete use [23 - 26]. Tapered RCHBs are often used in simply bridges, structural portal frames for economic and creative appearance reasons. Probably the main problem with RCHB is the limited experimental studies dedicated to comprehension RCHBs behavior under flexure and shear loading conditions, where shear behavior was the main concern [27 - 34]. As a result, very limited experimental research studies focused on flexure and shear behavior of externally strengthening haunched beams of RCHBs with FRP are available in the literature [35, 36]. The ECC appears according to previous researches is an encouraging material for the application as complete or partial substitution of concrete in the tension region of beams subjected to flexural load due to desirable characteristic, excellent crack control, and solution of durability problems associated with the brittleness of concrete [37, 38]. Numerous studies have been conducted to investigate the effect of reinforced ECC -concrete composite prismatic beam [39 - 42]. While CFRP is effective in strengthening RC beams incorporating ECC as a layer around the main ECC beams [43]. This study aims to investigate the following: A) An effort to provide more experimental test data for self-compacting concrete haunched beams (SCCHBs) strengthened by externally bonded with unidirectional fabric CFRP and BFRP U-jacket strips, to evaluate and a better understanding of the effect of various FRP wrapping schemes on the structural shear and flexural behaviors. B) To study the (ECC) RHBs flexural behavior and strategy of ECC portions application in RHB members that are under comparatively high tensile stress for accomplishing the highest ECC cost to performance ratio in ECC/SCC RHBs series. C) And to study the influence of the U-CFRP strip anchorage strengthening system in improving RHBs performance by reducing flexural crack and prevent or delay debonding between contact layers for (ECC/SCC) composite haunched beams subjected to a flexural load.

2. Experimental Investigation work

The experimental work consists of the design and production 25 of RCHBs with a length of 1200mm, the effective span (L) of 1050mm, and a width of 120mm. The depth of beams is variable changing from 105mm (at each end) to 210mm (in the middle) linearly along the length of them. All RHBs were supported and tested under 4 points loading. The geometry, cross-sections, reinforcement details, and loading of shear and flexural specimens are illustrated in Fig. 1 (a) and (b), respectively.

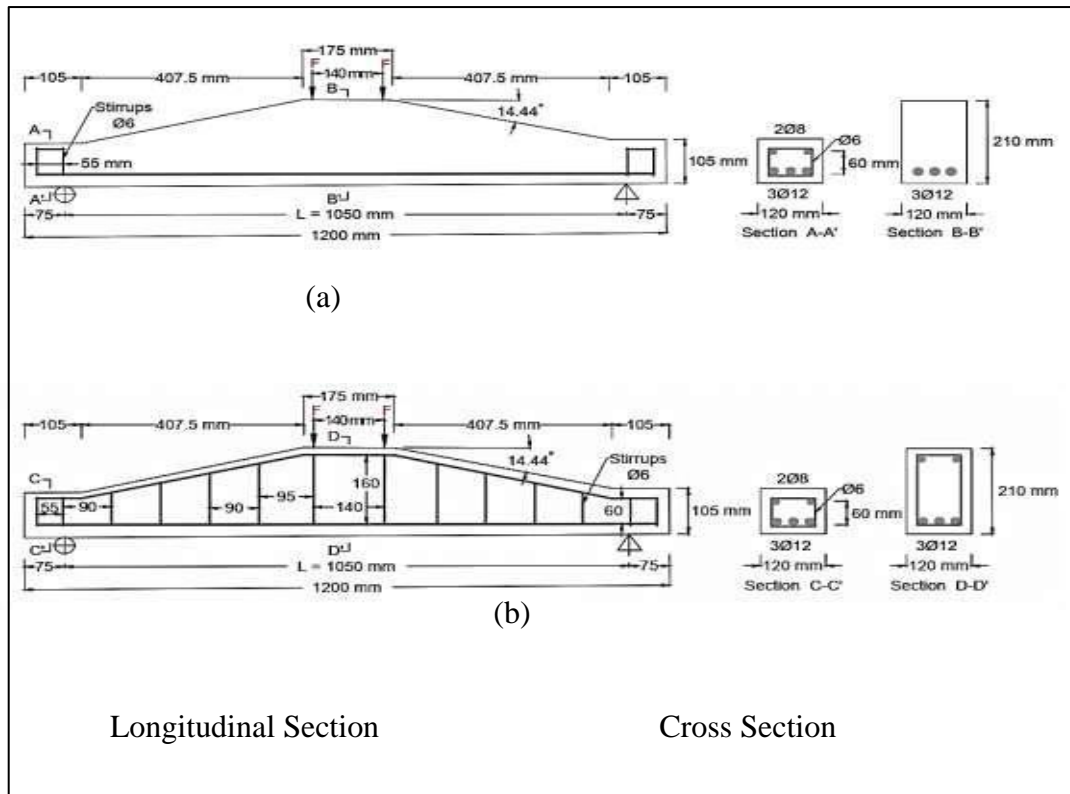


Figure 1. Detailing of tested specimens: (a) shear (RHBS); (b) flexural (RHBS)

All beams were longitudinally reinforced at the bottom with three steel deformed bars of 12 mm diameters, and the end of these bars were bent upward to prevent slip off them. The shear reinforcements were prepared with deformed bars having a 6 mm diameter. For the compression side of the haunched beams, two deformed bars of diameters 8 mm have been used. The measured mechanical properties of the steel reinforcements are listed in Table 1.

Table 1. Properties for the steel reinforcement

Bar diameter (mm)	f_{sy} (MPa)	f_u (MPa)	s_y
12	468	592	0.00234
8	550	640	0.00275
6	673	714	0.00336

For SCC, the concrete grade was C50/60. The materials used to produce the SCC mix were ordinary Portland cement 32.5R, crushed stone aggregate (gravel and sand) with an aggregate size of the gravel 11 mm, and the sand passed from sieve of 4 mm. The SCC mix proportions present in Table 2. The concrete compressive strength tests of cylinder samples (f_{cyl28}) have been carried out according to ASTM C39-96 [43] while the compressive strength tests of cube samples (f_{cu28}) have been performed according to BS 1881-116- 1983 [45]. The splitting tensile strength tests have been implemented according to ASTM C496 / C496M-11 [46, 47] to obtain f_{ct} , and modulus of elasticity (E_c) was evaluated using ASTM C469-02 [48]. The average measured strength values of the SCC at age of 28 days are summarized in Table 2.

Table 2. SCC mix proportions and strength characteristics

Cement (kg/m ³)	Sand (kg/m ³)	Gravel (kg/m ³)	Fly ash (kg/m ³)	Water (kg/m ³)	Super plasticizer (L/m ³)	Cube compressive strength f_{cu28} (MPa)	Cylinder compressive strength f_{cyl28} (MPa)	Modulus of elasticity E_c (GPa)	Tensile strength f_{ct} (MPa)
375	900	730	175	180	5	58.7	52.5	33	3.5

Moreover, investigations were conducted to study the mechanical behavior of ECC RHBs. Two mixes for conventional ECC M45 were prepared. One of the mixtures (MIX 2) is very similar to SCC regarding compressive strength. The main components of the first ECC mix (ECC MIX1) are ordinary Portland cement (32.5R), fly ash class (F) containing 4.24 % CaO, micro silica (Silica Fume) with an average grain size of 110 μm , poly vinyl alcohol (PVA) fiber (the fiber length is 8 mm and the diameter is 40 μm) and Super Plasticizer of HRWRA. In the second ECC mix (ECC MIX2), the main change was the adaptation of a combination of mineral admixtures (fly ash + slag) which can significantly increase the flexural strength, first cracking strength, and peaking strength of ECC [49]. Further details of the two ECC mixes are given in Table 3.

Table 3. Mix proportion of ECC (by weight) and Strength characteristics

Constituent	Cement	Silica Fume	Fly Ash	Slag	Water	Super Plasticizer (HRWRA)	PVA fiber (%)	f_{cu28} (MPa)	f_{cy18} (MPa)	E_c (GPa)	f_{ct} (MPa)
ECCMIX1	1	0.8	1.2	-	0.63	0.011	2.00	38	33	31.2	3.3
ECCMIX2	1	0.8	0.6	0.6	0.63	0.011	2.00	56	49	42	4.7

In the present research, two types of unidirectional CRFP and BFRP fabrics were used to study the behaviors of shear and flexural strengthening of haunched beams. The mechanical and physical properties of fabrics are given in Table 4.

Table 4. Fiber fabric mechanical and physical properties

FRP types	Tensile Strength (MPa)	Modulus of Elasticity (GPa)	Elongation (%)	Thickness (mm)	Area Weight (g/m^2)
CFRP	4900	240	2	0.3	300
BFRP	2100	105	2.6	0.3	300

Table 5 provides the technical data of the epoxy which was used for bonding the BFRP and CFRP fabrics on surfaces of RHBs.

Table 5. Epoxy technical data [50]

Product chemistry	
MasterBrace [®] SAT 4500 Comp A	Epoxy Resin
MasterBrace [®] SAT 4500 Comp B	Epoxy Hardener
Mixed density	1.02 kg/liter
Viscosity	1500-2500 mPa.s
Compressive strength TS EN 196 (7 days)	> 60 N/mm ²
Flexural strength TS EN 196 (7 days)	> 50 N/mm ²
Bonding strength to concrete (7 days)	> 3.0 N/mm ²
Application temperature	+5° C - +30° C
Pot life	30 minutes
Fully cured at 20 ° C	7 days

The moulds of specimens were prepared from plywood to obtain smooth surfaces. Haunched regions were obtained using trapezoidal plates designed according to the geometry of haunches. Additional measures were taken for RHBs containing ECC layers (ECC/SCC composite reinforced haunched beams) by fabrication of two removable plywood strips that can easily be removed after casting the ECC layer. The depth of ECC layers was 70 mm (one-third of the total depth), while two lengths were considered for ECC layers which were 200 mm (1/6 of total length) and 1200 mm (total length), respectively. To achieve optimum bonding strength, proper surface preparation is very essential during covering the beams. In the first step, the surfaces all RHBs wrapping with FRP surfaces were roughened by using both coarse sandpaper texture and a grinder machine. Then dust and dirty particles were cleaned from all treated RHBs by the air compressor. The bottom edges of RHBs were rounded and smoothed to reduce the stress concentration. In addition, all RHBs surfaces were required to be dried from any moisture. Then acetone was used to clean all RHBs bonding surfaces. Two-epoxy

components were mixed with a proportion of 100:34 (by weight), as provided by the manufacturer, and were applied to marked regions on RCHBs surfaces which will have been covered with FRP fabrics. Both CFRP and BFRP fabrics had been cut to the required dimensions and then were saturated with the epoxy adhesive before bonding on the RCHBs surface. FRP fabric strips were squeezed along the fiber direction by using a soft and thin metal spatula until the elimination of the trapped air bubbles and keeping the fiber fabric strips tight and wrinkle-free. The saturated acetone cloth was used in order to clear the RHBs surfaces from the excessive epoxy adhesive. After the covering process, all of the strengthened RHBs were left at room temperature for 7 days to attain the target strength of the epoxy. The strengthening program consisted of two groups (G1 & G2) of RHBs. All RCHBs series in groups (G1 & G2) were strengthened with one layer of unidirectional FRP (CFRP & BFRP) fabrics, and the direction of the fibers was oriented in the direction which is nearly or completely normal to the direction of expected crack patterns of RHBs. A combination of conventional approaches of FRP strengthening consisted of U-jacketing, side bonding, and complete wrapping was adopted according to fib Task Group 9.3-01 and ACI 440.2R-08 [51, 52]. Both FRP strips (strip width = 50 mm) and continuous fabric sheets can be used, and the fibers in the FRP strips may be oriented with different angles. The length of the FRP strengthening region was determined according to the length of the region in which the expected failure mode took place (for shear strengthening the length is, $SL= 450$ mm for each side of RCHBs, and flexural strengthening the length is, $L=1050$ mm). However, the U-shaped FRP fabric strips anchorage (anchorage strip width = 50 mm) methods were used to prevent debonding for the G2 group (flexural strengthening) of SCC RCHBs. Servo-hydraulic and displacement controlled testing machine was used for loading tests of all RHBs specimens as shown in Fig. 2. The hydraulic jack in the loading device controls the load increment on test specimens, and the applied load measures via a 600 kN capacity load cell installed in the machine. Each RHB was loaded until failure by four-point loading tests with a span length of 1050 mm (one of the supports was free to rotate around the transverse direction, while the other one was not). The displacement was progressively increased with a rate of 0.2mm/min by using the hydraulic displacement sensor inside the loading machine. Measurements of vertical deflections were recorded via linear variable displacement transducers (LVDT) to determine the mid-span deflection. All measurements were automatically collected and recorded by a data acquisition system and stored in a computer. During the processing of loading, the crack propagation on each tested specimen was immediately followed and marked.

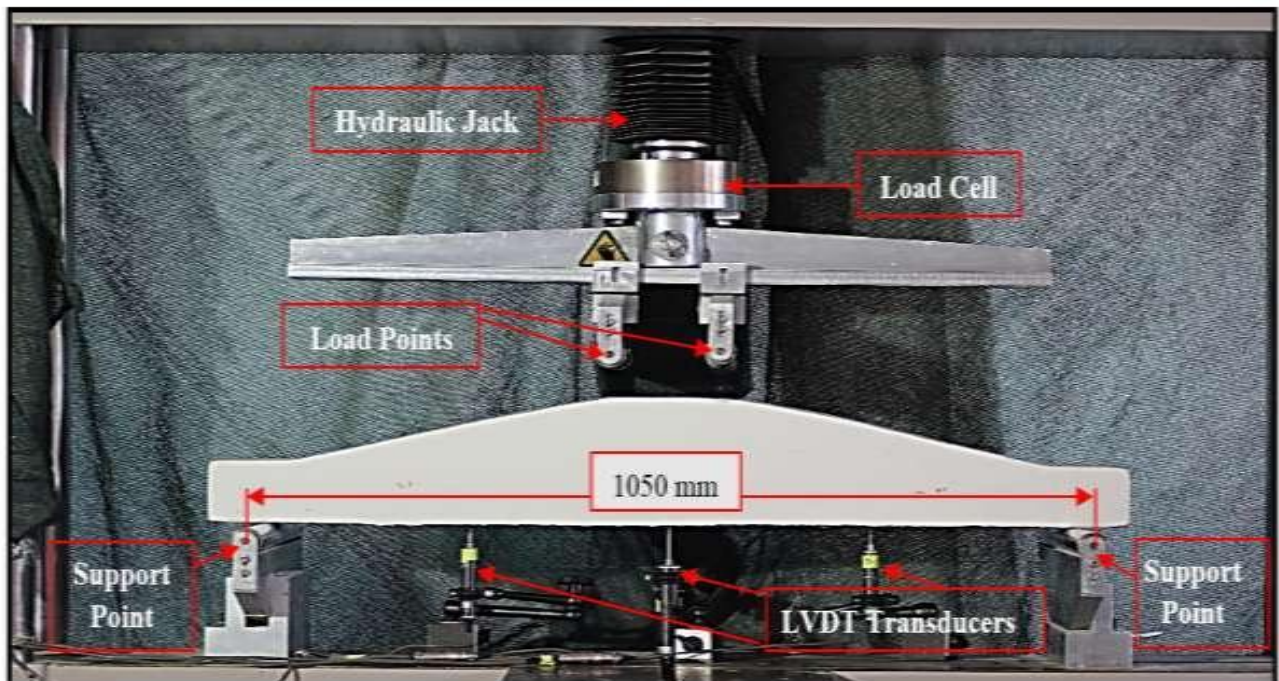


Figure 2. Testing installation arrangements of haunched beams specimens.

Experimental program including the strengthening details of three series of RHBs and details of series are given in Table 6. Each series was produced from different materials. The first RHB series consisted of SCC. The second series contained both SCC and ECC layers. The third series included only ECC. The strengthening schemes are illustrated in Appendix A Fig. S.1, 2, and 3.

Table 6. Details of RH beam specimens

Group	Beam type	Specimen symbols	Strengthening type	Strengthening material	Description of beam details	Strengthening scheme
G1 (Shear Strengthening)	S1: SCC	CS	----	----	Shear Control Beam, No Strengthening	Fig.S.1a
	S1: SCC	SC1	(S)	CFRP	U-shape strips with one layer of width 50 mm 90° direction spaced at 100 mm c/c along length = (SL=450 mm) x 2	Fig.S.1b
	S1: SCC	SB1	(S)	BFRP	U-shape strips with one layer of width 50 mm 45° direction spaced at 100 mm c/c along length = (SL=450 mm) x 2	Fig.S.1c
	S1: SCC	SC2	(S)	CFRP	U-shape strips with one layer of width 50 mm 45° direction spaced at 100 mm c/c along length = (SL=450 mm) x 2	Fig.S.1d
	S1: SCC	SB2	(S)	BFRP	U-shape strips with one layer of width 50 mm 45° direction spaced at 100 mm c/c along length = (SL=450 mm) x 2 + side strips along edge shear crack	Fig.S.1e
	S1: SCC	SC3	(S)	CFRP	Wrap Strengthening along all path length of diagonal shear crack which cracks pattern obtained from tested shear control beam as shown in (Fig.9A (a))	Fig.S.1f
	S1: SCC	SB3	(S)	BFRP	Full U-shape wrap along length = (SL =450 mm) x 2	Fig.S.1f
	S1: SCC	SC4	(S)	CFRP		
	S1: SCC	SB4	(S)	BFRP		
	S1: SCC	SC5	(S)	CFRP		
	S1: SCC	SB5	(S)	BFRP		
G2 (Flexural Strengthening)	S1: SCC	CF	----	----	Flexural Control Beam, No Strengthening	Fig.S.2a
	S1: SCC	FC1	(F)	CFRP	One layer of width 120 mm of CFRP fabric was applied along the bottom length between supports of the beam = (L= 1050 mm) without end anchorage	Fig.S.2b
	S1: SCC	FC2	(F)	CFRP	One layer of width 120 mm of FRP fabric was applied along the mid-span bottom length of the beam = (1/6 TL= 200 mm) + with Two U - shape strips end anchorage of 50 mm width	Fig.S.2c
	S1: SCC	FB2	(F)	BFRP	One layer of width 120 mm of FRP fabric was applied along the bottom length between supports of the beam = (L= 1050 mm) + with Four U-shape strips end anchorage of 50 mm width	Fig.S.2d
	S1: SCC	FC3	(F)	CFRP	One layer of full U-shape wrap of FRP fabric was applied along the length between supports of the beam= (L =1050 mm)	Fig.S.2e
	S1: SCC	FB3	(F)	BFRP		
	S1: SCC	FC4	(F)	CFRP		
G2 (Flex)	S2:Co mp. ECC/S	EC1	(F)	CFRP	Composite ECC/SCC RHB, which consisted of ECC layer with depth = (1/3 mid-span depth of	Fig.S.2f

Group	Beam type	Specimen symbols	Strengthening type	Strengthening material	Description of beam details	Strengthening scheme
Flexural-Full	CC				RHB) =70 mm were applied along the mid-span bottom length of the beam = (1/6 TL= 200 mm) + with Two CFRP fabric U-shape strips end anchorage of 50 mm width.	Fig.S.3a
	S2: Comp. ECC/S CC	EC2	(F)	CFRP	Composite ECC/SCC RHB, which consisted of ECC layer with depth = (1/3 mid-span depth of RHB) =70 mm were applied along the bottom length between supports of the beam = (L= 1050 mm) + with Four CFRP fabric U-shape strips end anchorage of 50 mm width	Fig.S.3b
	S2: Comp. ECC/S CC	E1	----	----	No Strengthening, Composite ECC/SCC RHB, which consisted of ECC layer with depth = (1/3 mid span depth of RHB) =70 mm were applied along the mid-span bottom length of the beam = (1/6 TL= 200 mm)	Fig.S.3c
	S2: Comp. ECC/S CC	E2	----	----	No Strengthening, Composite ECC/SCC RHB, which consisted of ECC layer with depth = (1/3 mid span depth of RHB) =70 mm were applied along the bottom length between supports of the beam (L= 1050 mm)	Fig.S.3d
	S3: ECC (MIX1)	E3	----	----	ECC RHB , No Strengthening	Fig.S.3d
	S3: ECC (MIX2)	E4	----	----	ECC RHB , No Strengthening	Fig.S.3e

3. Results and discussion

3.1. Shear strengthening group (G1)

RHBs of this group was designed to obtain shear failure in the unstrengthened phase. The control beam of this group was designated as CS, and its crack pattern and failure mode. Table 7 and Fig. 3 summarizes the results of the first cracking load ($P_{Cr/s}$) and the ultimate test load ($P_{u/s}$). Table 7 shows the mid-span deflections regarding first cracking and ultimate loads Cr/S, u/S, respectively for all testing of the G1 group. As explained in Table 7, similar SF modes because of suddenly arisen diagonal cracks between the earnest loading point to the support point were observed for all RCHBs in the group. According to all failure modes and test results of the shear strengthening group (G1), it is obvious that the shear diagonal cracks of strengthened RCHBs are always followed by debonding and/or rupture of the FRP fabrics, as shown in Table 7. In addition, strengthening of RCHBs by FRP fabrics led to a significant increase in the first crack load and ultimate shear load capacity for all strengthening cases compared to the CF. Furthermore, strengthened specimens exhibited warning signs like snapping sounds before failure. Increases in the first crack load of RCHBs strengthened with CFRP fabric were 62.6%, 18.1%, 53.5%, 67.5%, and 38.1% for strengthening schemes of SC1, SC2, SC3, SC4, and SC5, respectively, while increases in ultimate load capacity for the same strengthening schemes were 59.4%, 17.4%,

50.8%, 72.8%, and 36.5%, respectively. In the case of RCHBs strengthened with BFRP fabrics, increases in the first crack loads were 35.4%, 7.1%, 16.9%, 66.7%, and 13.9% for strengthening schemes of SB1, SB2, SB3, SB4, and SB5, respectively, while increases in the ultimate loads were 32.6%, 7.6%, 17.3%, 71.4%, and 14.6%, respectively. Effects of FRP fabric types (CFRP and BFRP fabric) on the mechanical behavior of RHB beams are shown in Figs 4 to 8 in terms of deflection load and ultimate shear capacity for each strengthening scheme. Type and location of the failures occurred in the strengthened RHBs. It can be concluded from the results that the lowest upgrade is obtained from the strengthening schemes of SB2 and SC2 (U-shape strips only which are 45o inclined). However, this strengthening scheme can be improved by the addition of FRP strips along the inclined edges of RHBs. For instance, initial crack loads and ultimate loads of SB3 and SC3 were high as compared to loads of SB2 and SC2. However, this improvement is higher for strengthening with CFRP fabric (30% and 28.4% for initial crack and ultimate loads, respectively). Furthermore, the addition of edge strips along inclined edges in addition to inclined U-shaped strips provided an anchorage effect on the end of the U-shaped strips which retards the formation of the first crack, crack propagation and so, failure. Another important improvement of the strips along the inclined edges was the prevention of debonding of U-shaped FRP strips. All these improvements also reduced the deterioration amount of the strengthened RHBs. According to the test results, it can be claimed that both of the FRP fabrics material type and arrangement of shear strengthening schemes cases factors are effective on the improvement of load capacity and deflection capability of the RCHBs as compared to the corresponding results of unstrengthened control specimen. Except for SC4 and SB4 specimens as shown in Fig. 7, in which the arrangement of shear strengthening FRP fabric scheme was the dominating factor in the improvement of load capacity and deflection capability of the RCHBs as compared to control beam.

Table 7. Shear strengthening tested RCHB specimen's results data and the failure scheme of final cracking.

Specimens symbols	$P_{Cr/S}$ (Load) (kN)	Cr/S Midspan deflection (mm)	$P_{u/S}$ (Load) (kN)	u/S Midspan deflection (mm)	Mode of failure	Failure scheme of the final cracking
CS	26.5	0.6251	70.235	1.865	SF	Fig. S.4.a
SB1	35.9	0.82	93.20	2.770	SF	Fig.S.4.b
SC1	43.1	1.125	111.96	3.685	SF	Fig.S.4.c
SB2	28.4	0.645	75.63	2.215	SF	Fig.S.4.d
SC2	31.3	0.905	82.46	2.675	SF	Fig.S.4.e
SB3	31.0	0.630	82.39	2.165	SF	Fig.S.4.f
SC3	40.7	40.7	1.019	105.96	SF	Fig.S.4.g
SB4	44.2	1.090	120.42	4.800	SF	Fig.S.4.h
SC4	44.4	1.641	121.41	4.671	SF	Fig.S.4.i
SB5	30.2	0.854	80.55	2.764	SF	Fig.S.4.j
SC5	36.6	1.275	95.93	3.445	SF	Fig.S.4.k

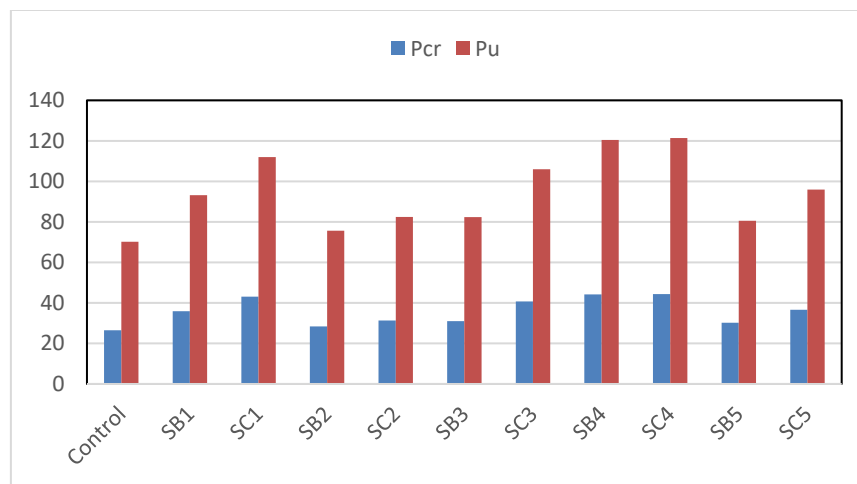


Figure 3. Effect of strengthening material type (CFRP and BFRP fabric) and strengthening scheme cases on initial and the ultimate cracking loads tested specimens

However, the most efficient strengthening configuration was obtained as a result of the fourth scheme which includes SC4 and SB4 specimens. This result is due to the adopted strengthening scheme in which the wrapped FRP fabrics in a manner that their fibers were almost completely normal to expected shear crack of the beams. The expected shear crack was predicted from the resulting crack pattern of the control specimen. The maximum percentage increases in ultimate shear failure load achieved by SC4 and SB4 specimens were about 72.8%, 71.4% for CFRP and BFRP fabric strengthening, respectively compared with the control beam. CFRP fabric, as a strengthening material, showed higher performance than BFRP fabric in the majority of strengthened specimens. The increase in ultimate load capacity for SC1, SC2, SC3, and SC5 specimens was higher as the amount of 20.1%, 9%, 28.6%, and 19%, respectively as compared to the increasing for SB1, SB2, SB3 and SB5 specimens. It is worthy to mention that there is almost no difference between ultimate load capacities of carbon and basalt fabric strengthened specimens regarding fourth strengthening scheme (SC4 and SB4) as demonstrated in Fig. 3.

3.2. Flexural strengthening group (G2)

This group consists of two-beam series (Series 1: SCC beams & Series 2: ECC/SCC composite beams) and contains a reference RH beam (control beam (FC)) for self-compacting beams series that are strengthened. In addition, two series of RHBs (E1&E2) were produced for Series 2: ECC/SCC composite beams to study the anchorage effect achieved by U-shaped FRP strips. Results of $P_{Cr/F}$, $P_{u/F}$, mid-span deflections related to first cracking and ultimate load Cr/F , u/F) and failure modes for all tested RHBs of group G2 are tabulated in Table 8 and shown in Fig. 9.

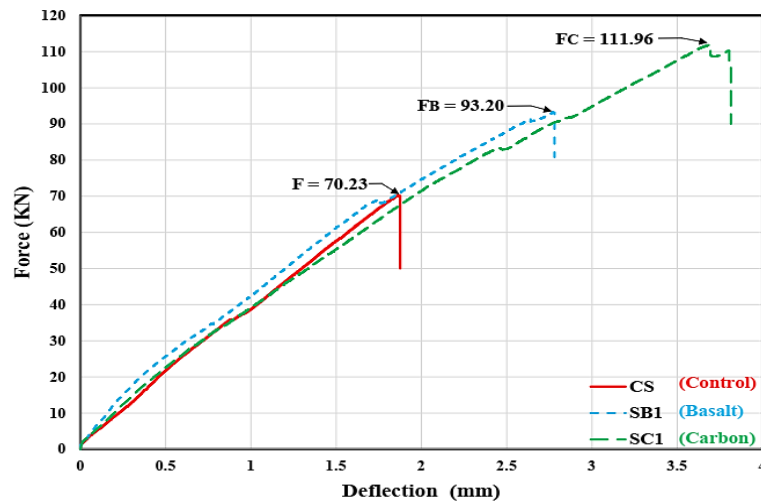


Figure 4. SC1 and SB1 specimens load of deflection.

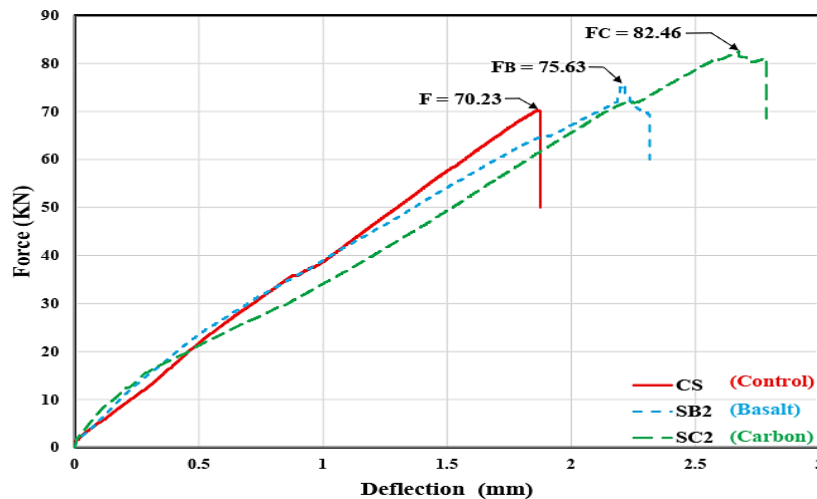


Figure 5. SC2 and SB2 specimens load of deflection.

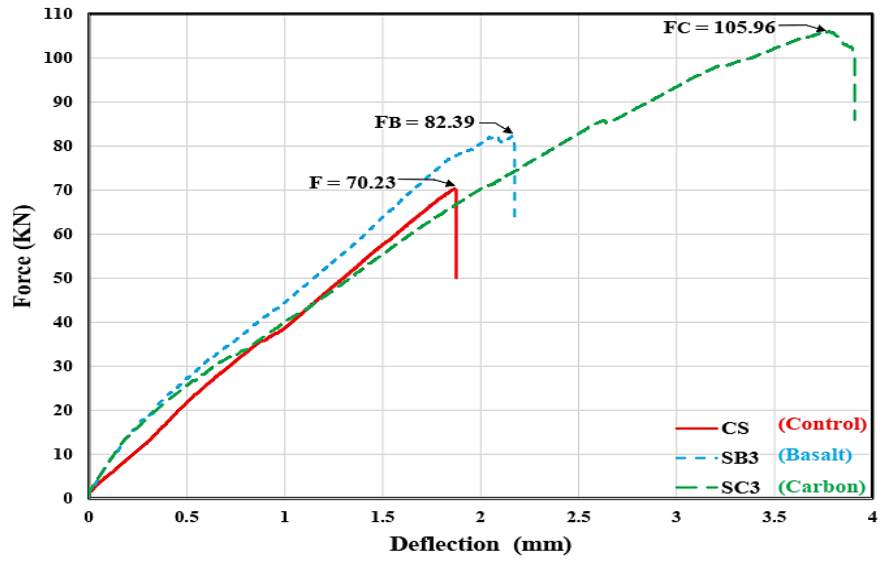


Figure 6. SC3 and SB3 specimens load of deflection.

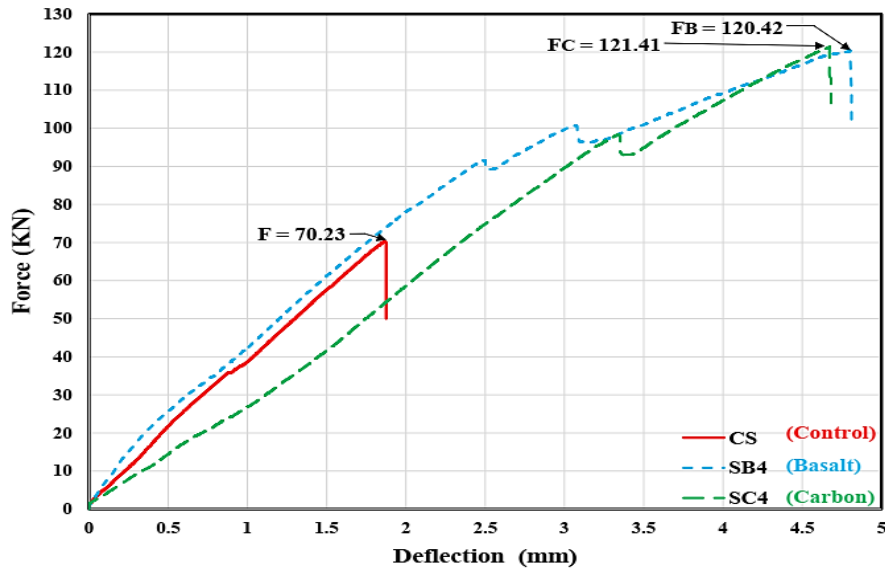


Figure 7. SC4 and SB4 specimens load of deflection.

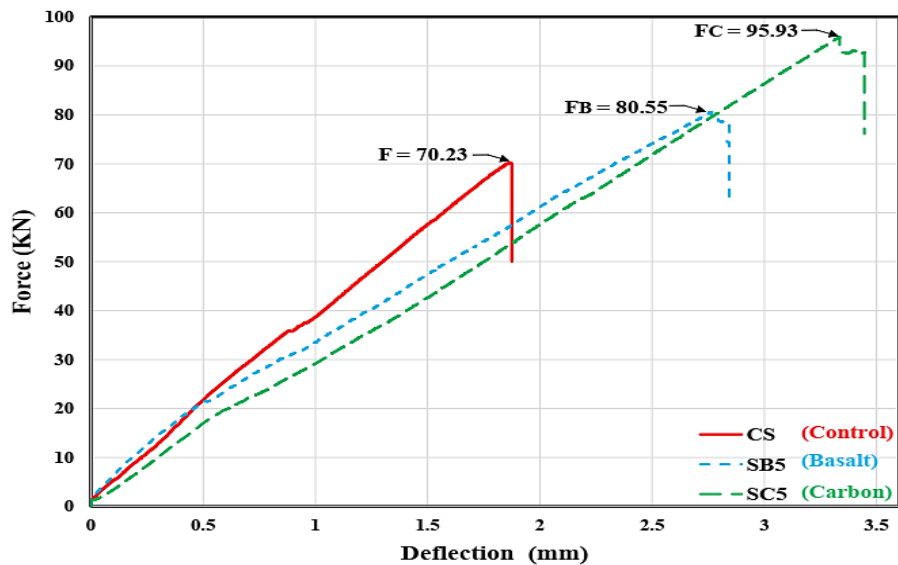


Figure 8. SC5 and SB5 specimens load of deflection.

The type of the first cracks taking place at the mid-span and tension face of tested specimens were pure flexure cracks for control beam (CF) and these cracks distributed along the tension face to the supports. The pure flexural cracks continued to form perpendicular to the flexural reinforcement bars up to 35-50 % of the ultimate load ($P_{u/F}$). Thereafter, some of the cracks along the shear span inclined to the loading points on both sides of the beams. For specimens of CF, FC1, FC2, FC3, E1, and EC1, the flexural cracks under the loading point were wider than other cracks at failure, and no observed concrete crushing in the compression zone after yielding flexural reinforcement. Some significant observations were monitored during crack propagation on all tested specimens, however, propagation of flexural cracks and yielding of the reinforcement followed by concrete crushing for specimens of FB2, FB3, E2, and EC2. For instance, vertical and inclined flexural cracks on beams were almost similar and occurred simultaneously during the test for both shear spans of the beams until failure. In addition, loading test results indicate that flexural strengthening of RCHBs via FRP fabrics significantly reduced the width of flexural cracks, but increasing the fine cracks consistently distributed along the beam span. Moreover, the formation and propagation of the flexure crack were slightly later in the strengthened SCC and ECC/SCC composite RHBs compared to the CF.

The maximum delays in the first flexure crack (the first crack load ($P_{Cr/F}$)) obtained in FC3 and EC2 specimens among strengthened SCC and ECC/SCC beams, respectively.

Table 8. Flexural strengthening tested RHB specimen's results data and final cracking failure scheme.

Specimens Symbols	Series No. Beam Type	$P_{Cr/F}$ (Lo) (kN)	Cr/F Midspan Deflection (mm)	$P_{u/F}$ (Load) (kN)	u/F Midspan Deflection (mm)	Mode of Failure	Final Cracking Failure Scheme
CF*	S1: SCC	30	0.590	139.5	11.892	FF*	Fig.S.5.a
FC1	S1: SCC	35	0.863	148	6.083	D# of CFRP followed by FF**	Fig.S.5.b
FC2	S1: SCC	32.5	0.912	158	32.672	R* followed by FC* followed CC\$	Fig.S.5.c
FB2	S1: SCC	33	0.85	147.5	14.69	FF* followed by CC\$\$.	Fig.S.5.d
FC3	S1: SCC	37	1.392	167.8	7.902	D## of CFRP followed by R** followed by FF**	Fig.S.5.e
FB3	S1: SCC	36	1.087	155.5	12.217	D# of BFRP followed by R* followed by CC\$.	Fig.S.5.f
FC4	S1: SCC	-	-	179.81	6.536	R* of CFRP followed by CC\$\$	Fig.S.5.g
FB4	S1: SCC	-	---	177.61	12.071	R** of BFRP followed by CC\$\$	Fig.S.5.h
E1	S2:Comp. ECC/SCC	33	0.3829	150	12.418	FC* followed by D### followed by FF**	Fig.S.5.i
E2	S2:Comp. ECC/SCC	38	0.439	152.3	11.942	FC* followed by D### followed by CC\$\$	Fig.S.5.j

Specimens Symbols	Series No. Beam Type	$P_{Cr/F}$ (Lo) (kN)	Cr/F Midspan Deflection (mm)	$P_{u/F}$ (Load) (kN)	u/F Midspan Deflection (mm)	Mode of Failure	Final Cracking Failure Scheme
EC1	S2:Comp. ECC/SCC	35	0.392	152	14.822	FZ followed by CC\$	Fig.S.5.k
EC2	S2:Comp. ECC/SCC	45	0.383	159	7.151	FF*, FZ followed by CC\$\$	Fig.S.5.1

FF*: flexure failure due to yielding of steel with wide cracks at mid-span.
 FF**: flexure failure due to yielding of steel.
 CC\$: crushing of concrete in compression zone under one of sideloads points.
 CC\$\$: crushing of concrete in compression zone between the two points of load application on beam.
 D#: Debonding of fabric.
 D##: Debonding of fabric bottom face strip on the right side of beam,
 D###: debonding around the edges of the contact between SCC and ECC layer
 R*: Rupture in of U shape CFRP fabric anchorage.
 R**: Rupture in fabric bottom face strips at mid-span.
 FC*: Increase in width of flexural cracks at mid-span.
 FZ: Flexure zone and without the appearance of Debonding between SCC and ECC layer edges.

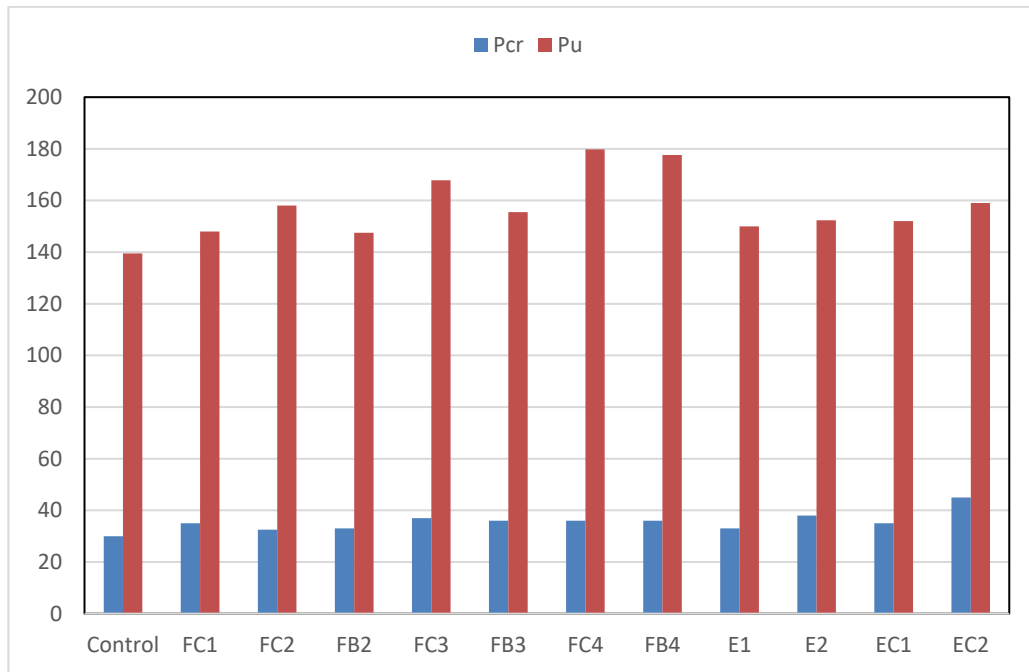


Figure 9. Effect of strengthening material type (CFRP and BFRP fabric) and the effect of flexural strengthening scheme cases on initial and ultimate cracking loads for both RHB series tested specimens

The effect of strengthening material type (CFRP and BFRP fabric) and the effect of flexural strengthening schemes (tension face and/or U-anchorage strengthening) on the improvement of the initial cracking loads and the ultimate loads are clearly illustrated in Table 8. The percentages of increase in the first crack load ($P_{Cr/F}$) are about 16.6%, 8.3%, 10%, 23.3%, 20%, 10%, 26.6%, 16%, 50% and the percentages of increasing in the ultimate load (P_u) are about 6.09%, 13.2%, 5.7%, 20.2%, 11.4%, 7.5%, 9.1%, 8.9%, 13.9% as compared with the control specimen for FC1, FC2, FB2, FC3, FB3, E1, E2, EC1 and EC2, respectively. The flexural strengthening program started by studying the effect of U-shaped anchorage achieved via FRP fabric strips at two locations, which are the region near to loading points and the region near to supports. As concluded from the results of shear strengthened RCHBs, since CFRP fabrics have superior mechanical performance and high effectiveness regarding delay of debonding as compared to BFRP fabrics, CFRP fabrics were adopted for the strengthening configurations containing U-shaped anchorage. According to the test results of FC1 and FC3 specimens, it can be noticed that anchorage with U-shaped FRP strips in addition to straight FRP fabric strips on tension face

significantly improves the flexural behavior of strengthened RCHB by preventing or delaying premature debonding of FRP strips on the bottom tension face which occurs due to excessive tensile stresses. This enhancing behavior led to the increasing in the ultimate load ($P_{w/F}$) as the amount of 13.3% & 20.2% as compared to FC1 specimen (strengthened without anchorage) and control beam (CF), respectively. However, it can be concluded that anchorage with U-shaped FRP strips reduces the ductility of strengthened RCHBs of group G2, while the failure is not brittle. The effect of strengthening material (CFRP & BFRP fabric) and the effect of length of FRP strips on bottom tension face ($1/6L$ and L) with U-shaped FRP strips anchorage are shown in Figs. 11 and 12. According to the figures, it is clear that these parameters have an enhancing effect on the flexural behaviors of RCHBs. In addition to prevention of premature bonding via U-shaped FRP anchorage, flexural load capacity increased as the amount of 20.2% and 13.2 % for CFRP strip length of L and $1/6L$ on bottom tension face, respectively. However, the increase in the load capacity was 11.4% and 5.7% for the BFRP strip length of L and $1/6L$, respectively. Moreover, it can be concluded from load-deflection curves of strengthened flexural specimens that even higher flexural load capacities were obtained via CFRP fabric strengthening, the beams strengthened via BFRP fabrics, and the unstrengthened beam exhibit more ductile behavior. In addition, the maximum value of the $P_{w/F}$ carrying capacity is due to the effect of strengthening material type was about 7.9%. Based on the results, the highest increase in the $P_{w/F}$ value is obtained as a result of this strengthening scheme (complete covering with FRP fabric), which were 28.8% and 27.2% for CFRP and BFRP fabrics covering (FC4 and FB4 specimens), respectively. Also, the beam strengthened of CFRP (FC4) covering exhibited more ductile behavior as compared to BFRP covering for this strengthening scheme. Moreover, the covered beam by BFRP (FB4) fabric completely failed suddenly. Interestingly, the result is reversed with the result obtained from strengthening schemes of 2 and 3 (FB2, FC2, FB3, and FC3 specimens). This outcome can be attributed to the combination of the superior performance of CFRP fabric as compared to BFRP fabric regarding ultimate strength and increase in the amount of FRP fabrics in tension zone (FRP fabrics on the side of the beams in addition to the FRP strips on bottom tension face). This combination converts the region of rupture of CFRP fabric from the bottom tension face to side tension face causing ductile behavior and prevention of sudden failure. The failures were due to FRP rupture along both sides of the beam near the bottom face for specimens strengthened with BFRP fabric and FRP rupture at mid-span only for all sides of the beam for specimens strengthened with CFRP fabric. These ruptures were followed by the crushing of concrete in the compression zone located between two points of load application.

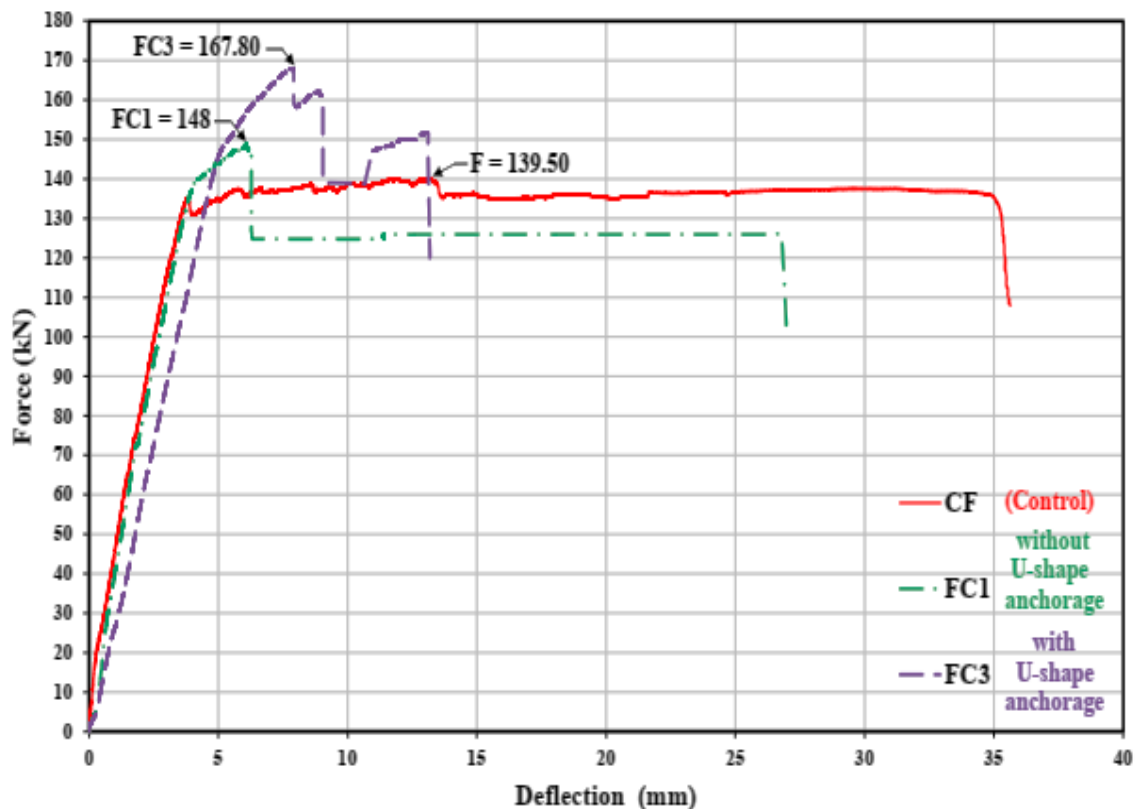


Figure 10. Effect of U-shape anchorage on the load-deflection curves of tested specimens FC1 & FC3

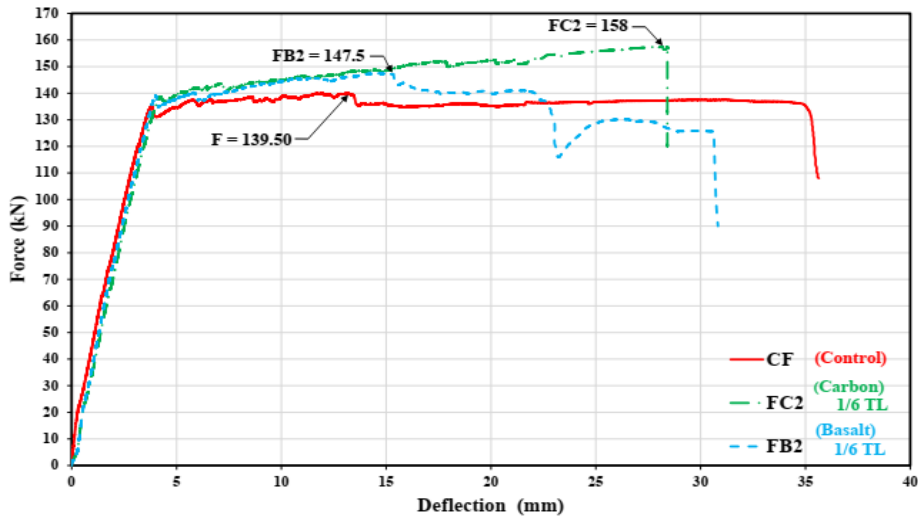


Figure 11. Effect of strengthening material type parameter and the effect of length of bottom face strengthening parameter (for length layer =1/6 TL) on the load-deflection curves of FC2 and FB2 tested specimens

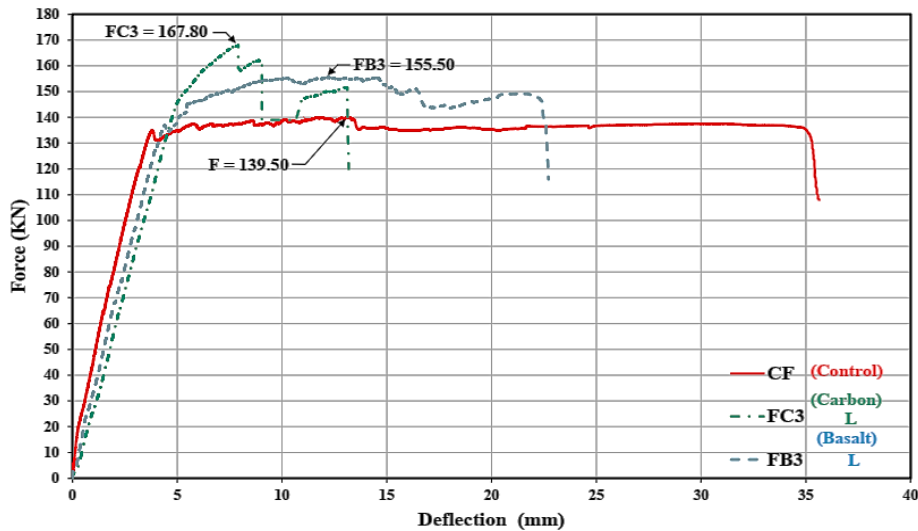


Figure 12. Effect of strengthening material type parameter and the effect of length of bottom face strengthening parameter (for length layer =TL) on the load-deflection

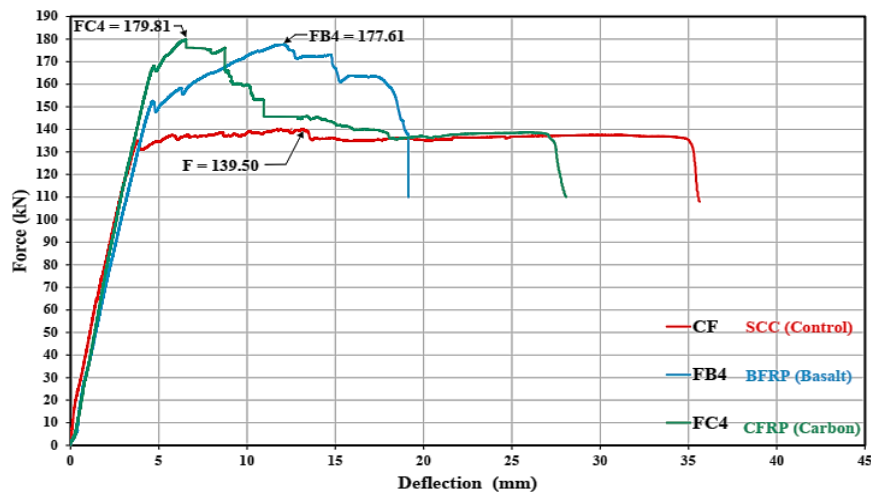


Figure 13. Effect of strengthening material type and full U-warping strengthening on the FC4 and FB4 specimens load of deflection.

The second tested RHB series (series2) in the present experimental program is ECC/SCC composite RHB, which contains the ECC layer in the tension zone. The second mixture of ECC (Mix 2) stated in Table 3 which adopted for the ECC layer. In addition, the effect of length of the ECC layer on the mechanical behavior of strengthened RHBs was investigated for accomplishing the highest ECC cost to performance ratio. Moreover, a possible contact problem between ECC and SCC layers was foreseen. The U- shape anchorage with CFRP fabric was also investigated for RHBs of this series to prevent premature failure. The U-shape anchorages were provided from CFRP fabric due to their superior performance as compared to BFRP fabric.

The effects of the ECC layer on the mechanical behavior of ECC/SCC composite haunched beams are shown in Figs. 14 and 15. It is clear that the ECC layer has an enhancing effect on the flexural behavior of the composite RHBs regarding ductility and load capacity, and also the degree of improvement is related to the ECC layer length. As the layer length increases, the first crack ($P_{Cr/F}$) delayed and the ultimate load capacity ($P_{u/F}$) significantly increased compared to the CF (type SCC) (CF, without ECC layer). The percentages of increase in ultimate load (P_u) were about 9.1% and 7.5% for E2 (ECC layer length is TL) and E1 (ECC layer length is 1/6TL) specimens, respectively as compared to CF. From the crack patterns of E2 and E1 specimens, it can be noticed that the stresses and cracks developed at the contact layer between ECC and SCC attempt to debond the ECC layer, and consequently premature failure happens. However, this problem can be solved by providing U-shaped anchorage from CFRP fabric. Using the U-shaped anchorage in EC2 and EC1 specimens increased the ultimate load ($P_{u/F}$) by about 14% & 9 %, respectively as compared to the CF.

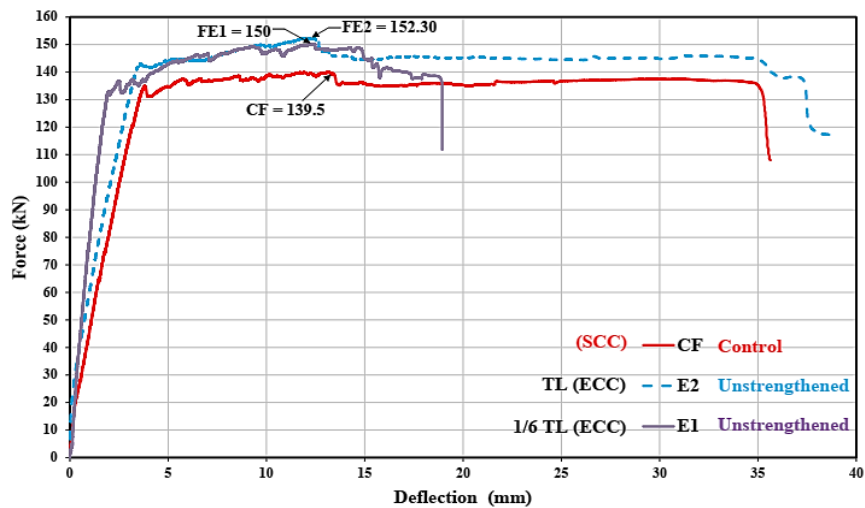


Figure 14. Effect of ECC layer length parameter (1/6 TL, TL) on the load-deflection curves of tested composite haunched beams specimens E1 and E2

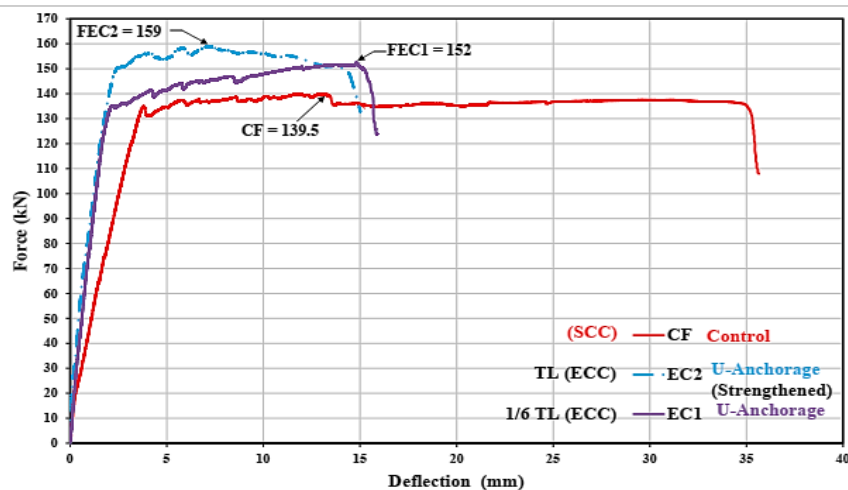


Figure 15. Effect of U-anchorage strengthening parameter on the load-deflection of tested composite haunched beams specimens EC1 and EC2

The increase was about 4.4%, 1.3% as compared to E2 and E1 specimens without U-jacket anchorage. In addition, it is apparent from test results that the U-shaped anchorage strengthening technique prevented and delayed the cracks formation and propagation at the contact layer between ECC and SCC, which increases bonding and load capacity. However, it can be concluded that the ductility of composite specimens without U-shaped anchorages (E1 and E2) was higher than the specimens having the anchorage (EC1 and EC2).

3.3. Flexural behavior of ECC reinforced haunched beams

The flexural behavior of haunched beams entirely produced from ECC via comparison with the behaviors of ECC haunched beam and ECC composite haunched beams have been studied to accomplish the best ECC cost to performance ratio strategy. Table 9 summarizes the test results data and cracking failure schemes which illustrates clearly the effect of different ECC mixes on the mechanical behavior of RHBs test specimen. The effect of each ECC mix was shown in Fig. 16. The first cracks were pure flexural cracks taking place at the middle and bottom of the specimens (E3 and E4). Thereafter, the pure flexure cracks continued to form perpendicular to the flexural reinforcement bars and evenly distributed along the tension side until the ultimate load ($P_{u/F}$). However, the regions near to supports where the cracks tended to be inclined flexure-shear cracks were up to 60% of the ultimate load ($P_{u/F}$). In addition, the cracks were symmetric on both sides of the beam until the main flexural cracks under the loading point became much wider than other cracks. However, for the E4 specimen, the cracks were tiny, randomly distributed at the bottom tension region and the number of cracks was less than the amount of E3 specimen up to 67 % of the ultimate load ($P_{u/F}$).

Table 9. Flexural strengthening tested ECC RHB specimen's results data and final cracking failure scheme

Specimens Symbols	Series No. & Beam Type	PCr/S (Load) (kN)	Cr/F Midspan Deflection (mm)	Pu/F (Load) (kN)	u/F Midspan Deflection (mm)	Final Cracking Failure Scheme
E3	S3: ECC MIX2	37.5	1.81	160	15.68	Fig.S.6.a
E4	S3: ECC MIX1	32	0.554	147.6	14.017	Fig.S.6.b

After that, the speed rate of crack propagations increased until the main flexural cracks under the loading point area became much wider than other cracks. Finally, all of the beams failed in the flexural mode as expected. However, the deterioration amount of the E4 specimen was higher than the amount of the E3 specimen regarding load capacity and crack formation. According to Table 9, the maximum percentage of increase in the first crack load ($P_{Cr/F}$) was about 25%. It is observed that the E3 specimen, in comparison to SCC control beam (CF) and the percentages of increase in ultimate load ($P_{u/F}$) were about 14.69 % and 5.8 % for E3 and E4 specimens, respectively.

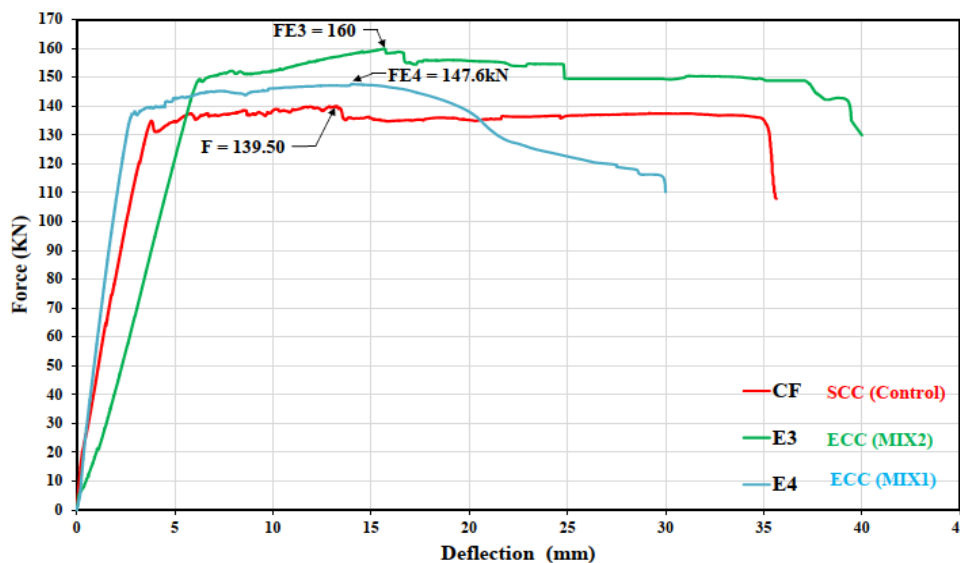


Figure 16. Effect of material mixes components on the curves of deflection load for ECC haunched beams tested specimens E3 and E4

The effects of both various strengthening techniques and various materials on the mechanical behavior of RHBs are shown and summarized in Figs. 17 and 18 in terms of load-deflection curves. It can be concluded that the increase in the length of the ECC layer led to increase in ductility and load capacity of RHBs. Furthermore, as shown in Figs. 17 and 18, the U-shaped anchorage via FRP fabrics decreased the ductility of strengthened SCC RHBs and ECC/SCC composite. However, as the length of strengthening materials (FRP fabrics or ECC layer) increased, the load capacity also increases for these beams.

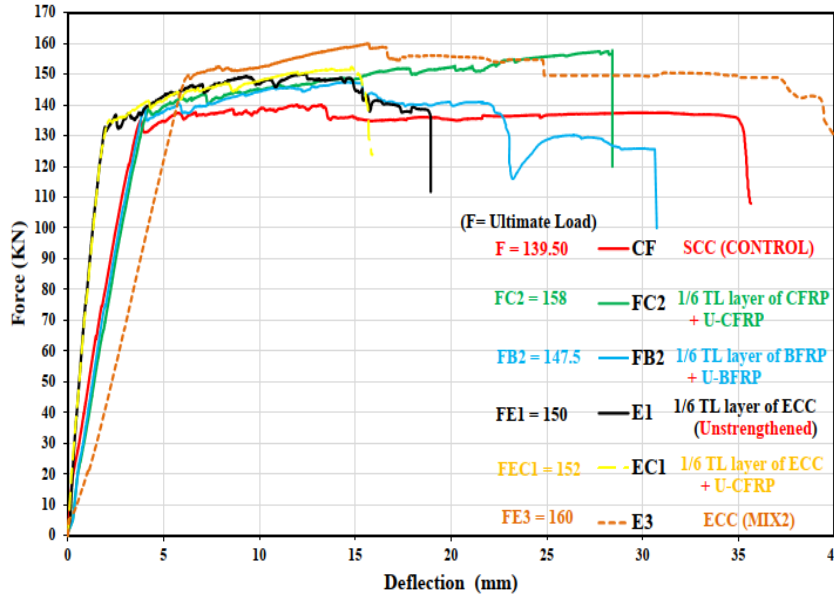


Figure 17. Both effects of fabrication materials of (RHBs) and strengthening (for layer length = 1/6 TL of the beam) technics cases on the curves of deflection load and the ultimate loads of tested specimens

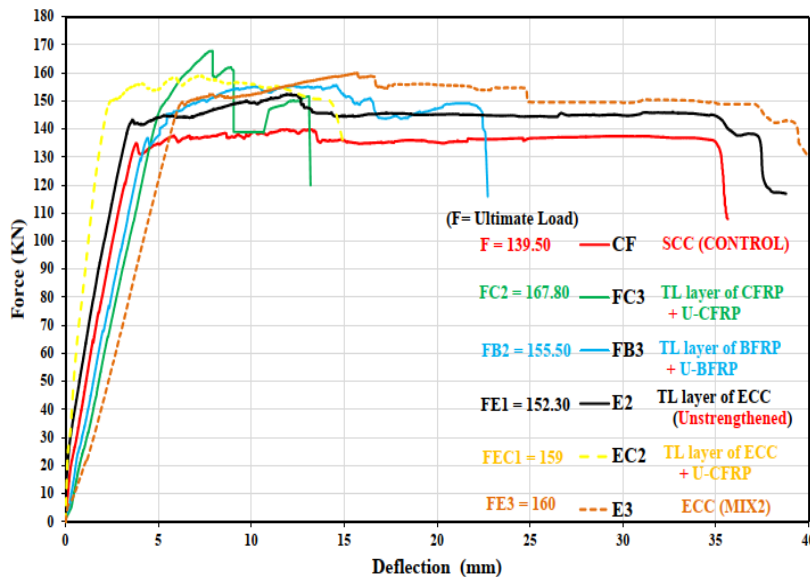


Figure 18. Both effects of fabrication materials of (RHBs) and strengthening (for layer length = L & TL of the beam) technics cases on the load-deflection curves and the ultimate loads of tested specimens

4. Conclusions

The point of the study was to look at the strengthening of RCHBs via CFRP and BFRP by the consideration of different strengthening configurations. RCHBs with and without shear reinforcement was included in the study as two strengthening groups (G1 and G2 groups). In addition, the present study investigated the mechanical behavior of RHBs produced from partially and/or entirely produced from ECC by taking the ECC portion length and U-shaped anchorage via FRP fabric into consideration. Strengthening configurations were determined

according to the expected failure modes of each group. Experimental work was conducted to achieve the objective of the study. Based on ultimate load capacities, load-displacement curves, crack patterns, and failure modes of twenty-five specimens' results; it can conclude the following:

The strengthening material type factor significantly influences the mechanical performance of strengthened RCHBs. CFRP fabrics have superior performance as compared to BFRP fabrics regarding load capacity. The highest difference between the load capacity of the beams strengthened with CFRP fabric and the capacity of the beams strengthened with BFRP fabric was 28.6% for the RCHBs without shear reinforcement (G1 group-between SC3 and SB3 specimens). The difference was 7.9% for the RCHBs with shear reinforcement (G2 group-between FC3 and FB3 specimens). The strengthening scheme factor was found to have a considerable influence on the load-carrying capacity of strengthened SCC RCHBs. In the shear strengthening group (G1), the best strengthening performance was obtained when FRP fabrics were placed orthogonal to the direction of the main diagonal shear crack and cover the expected path of the shear crack along a shear span of RCHBs (SC4 and SB4 specimens). The amounts of increase in the first crack load and ultimate shear load carrying capacity of by SC4 and SB4 specimens were about 72.8 %, 71.4 %, respectively as compared to the unstrengthened beam. While in the flexural strengthening group (G2), complete U covering of RCHBs with FRP fabrics (FC4 and FB4 specimens) was found to be the most efficient regarding load capacity. The amount of increase in the flexural load capacity of FC4 and FB4 specimens was 28.8% and 27.3%, respectively as compared to the unstrengthened specimen. The strengthening of SCC RHBs without stirrups (G1) by FRP fabrics was accompanied by additional ductile behavior (increase in deformation response) exhibiting warning signs like snapping sounds and/or debonding of the FRP fabric. In flexural strengthening (Group 2), in general results of crack patterns of the specimens showed that the strengthening with FRP fabrics reduced the crack width and increased the number of fine cracks distributed equally along the RCHB span. The application of U-jacket anchorage strengthening via FRP fabric (FC3 and FB3 in Group 2) was found to be effective regarding the delay and prevention of premature debonding of FRP fabrics from the bottom tension face and upgrading stiffness of strengthened beams. The maximum increases in ultimate load capacity of FC3 specimen were 20.2% and 13.37% as compared to unstrengthened beam and the beam strengthened without anchorage (FC1), respectively. However, the U-shaped anchorage with FRP fabric decreased ductility and the amount of decrease was higher when the anchorage was achieved by CFRP fabric. For ECC/SCC composite RHBs series, the use of U-shaped anchorage in EC2 and EC1 specimens increased the ultimate load ($P_{u/F}$) by about 14% & 9 %, respectively as compared to the CF. The increase was about 4.4%, 1.3% as compared to E2 and E1 specimens, which do not have U-jacket anchorage. However, the anchorage decreased the ductility of the beams. In most cases, strengthened RHBs having the anchorage failed due to debonding and/or FRP rupture followed by concrete crushing. The ultimate flexural load capacity of SCC RHBs of Group 2 increased as the length of FRP strip length on the bottom tension face increased from 1/6 TL to L, where TL and L were total length and length between supports of the beam, respectively. For instance, the load capacity of FC2 (1/6 TL) and FC3 (L) were higher as the amount of 13.2% and 20.2%, respectively, as compared to the CF, while this increase was 5.7% and 11.4% for FB2 (1/6 TL) and FB3 (L) specimens, respectively. The enhancing effect on the flexural performance response and the ultimate load capacity of ECC/SCC composite RHBs series (Group 2: beam Series 2: MIX2) increased, as ECC layer length increased. The increases in load capacity were 7.5% and 9.1% as compared to CF (SCC) for E1 (ECC layer length was 1/6TL) and E2 (ECC layer length was TL) specimens, respectively. RHBs, which were entirely produced from ECC, exhibited effective mechanical behavior regarding flexural performance, ductility, and load capacity. The acceptable results were observed for RHBs belonging to both ECC mixes considered in the study (MIX 1 and MIX 2). According to test results, the maximum percentage of increase in the first crack load ($P_{Cr/F}$) was about 25%, observed in the E3 specimen, as compared to the CF (SCC). Also, the percentages of increase in ultimate load ($P_{u/F}$) were about 14.69 % and 5.8 % for E3 and E4 specimens, respectively. According to specimen test results, the best-adopted strategy which contributed to understanding the ECC cost/performance ratio demonstrated the improved performance and load-carrying capacity of about 14.69 %. It is achieved by using full casting ECC RHB structural member (E3 specimen; MIX2) which can almost be obtained by the ECC/SCC composite RHB specimen (EC2:MIX2) of about 14% strengthened with U-jacket anchorage. However, a considerable loss in ductility was observed.

References

- [1] A. Belarbi, S. W. Bae, and A. Brancaccio, "Behavior of full-scale RC T-beams strengthened in shear with externally bonded FRP sheets," *Construction and Building Materials*, vol. 32. pp. 27–40, 2012.

- [2] H. Saeed Muhammed, N. Moneem Al Abdaly, H. Ali Zeini, and A. H. Saeed, "Use of polypropylene ropes in concrete to minimize steel reinforcement," *Period. Eng. Nat. Sci.*, vol. 7, no. 4, p. 1904, 2019.
- [3] A. Yazdanbakhsh and L. C. Bank, "The effect of shear strength on load capacity of FRP strengthened beams with recycled concrete aggregate," *Constr. Build. Mater.*, vol. 102, pp. 133–140, 2016.
- [4] P. Alagusundaramoorthy, I. E. Harik, and C. C. Choo, "Flexural Behavior of R/C Beams Strengthened with Carbon Fiber Reinforced Polymer Sheets or Fabric," *J. Compos. Constr.*, vol. 7, no. 4, pp. 292–301, 2003.
- [5] F. Ceroni, "Experimental performances of RC beams strengthened with FRP materials," *Construction and Building Materials*, vol. 24, no. 9, pp. 1547–1559, 2010.
- [6] M. Mahal, B. Täljsten, and T. Blanksvärd, "Experimental performance of RC beams strengthened with FRP materials under monotonic and fatigue loads," *Construction and Building Materials*, vol. 122, pp. 126–139, 2016.
- [7] M. Jaiswal, and G. Ramtekkar, "Experimental Study of Reinforced Concrete (RC) Beams Strengthened by Carbon Fiber Reinforced Polymer (CFRP): Effect of Beam Size and Length of CFRP", *International Journal of Applied Engineering Research*, vol. 12, no. 24, pp. 14075-14081, 2017.
- [8] B. Täljsten, "Strengthening of concrete structures for shear with bonded CFRP fabrics" *Proceedings of US- Canada-Europe Workshop on Bridge Engineering, EMPA, Zurich, Switzerland*, pp. 57-64. 1997
- [9] B. Täljsten, "Strengthening concrete beams for shear with CFRP sheets," *Construction and Building Materials*, vol. 17, no. 1, pp. 15–26, 2003.
- [10] G. Kim, J. Sim, and H. Oh, "Shear strength of strengthened RC beams with FRPs in shear," *Constr. Build. Mater.*, vol. 22, no. 6, pp. 1261–1270, 2008.
- [11] A. K. AL-Asad, M. Muttashar, and A. L. Almutairi, "Modelling reinforced concrete beams for structural strengthening of buildings," *Periodicals of Engineering and Natural Sciences*, vol. 8, no. 2, pp. 1083–1095, 2020.
- [12] A.C. Institute, *Building Code Requirements for Structural Concrete (ACI 318-14): Commentary on Building Code Requirements for Structural Concrete (ACI 318R-14): an ACI Report.*: American Concrete Institute. ACI, 2014.
- [13] A. ur R. Khan and S. Fareed, "Behaviour of Reinforced Concrete Beams Strengthened by CFRP Wraps with and without End Anchorages," *Procedia Eng.*, vol. 77, pp. 123–130, 2014.
- [14] G. Spadea, F. Bencardino, F. Sorrenti, and R. N. Swamy, "Structural effectiveness of FRP materials in strengthening RC beams," *Eng. Struct.*, vol. 99, pp. 631–641, 2015.
- [15] H.V. GangaRao, and P. Vijay, "Bending behavior of concrete beams wrapped with carbon fabric", *Journal of structural engineering*, vol. 124, no. 1, pp. 3-10, 1998.
- [16] O. Chaallal, M.-J. Nolle, and D. Perraton, "Shear strengthening of RC beams by externally bonded side CFRP strips", *Journal of composites for construction*, vol. 2, no. 2, pp. 111-113, 1998.
- [17] H. A. Abdalla, A. M. Torkey, H. A. Haggag, and A. F. Abu-Amira, "Design against cracking at openings in reinforced concrete beams strengthened with composite sheets," *Composite Structures*, vol. 60, no. 2, pp. 197–204, 2003.
- [18] C. Pellegrino, and C. Modena, "Fiber-reinforced polymer shear strengthening of reinforced concrete beams: Experimental study and analytical modeling", *ACI Structural Journal*, vol. 103, no. 5, pp. 720, 2006.
- [19] J. F. Dong, Q. Y. Wang, C. C. Qiu, and D. He, "Experimental Study on RC Beams Strengthened with CFRP Sheets," *Adv. Mater. Res.*, vol. 213, pp. 548–552, 2011.
- [20] F. Yuan, J. Pan, and C. K. Y. Leung, "Flexural Behaviors of ECC and Concrete/ECC Composite Beams Reinforced with Basalt Fiber-Reinforced Polymer," *J. Compos. Constr.*, vol. 17, no. 5, pp. 591–602, 2013.
- [21] R. Singaravadivelan, N. Sakthieswaren, and K. L. Muthuramu, "Experimental Investigation on the Behaviour of Flexural Strengthening of Beam Using Basalt Fiber," *International Conference on Automotive, Mechanical and Materials Engineering (ICAMME'2012) Penang (Malaysia)*. pp. 85–89, 2012.
- [22] I. Sfikas, "Self-Compacting Concrete: History & Current Trends," *Concr.*, vol. 51, pp. 12–16, 2017.
- [23] H. Okamura and M. Ouchi, "Self-Compacting Concrete, *Journal of Advanced Concrete Technology*, Vol.1, No.1, April 2003," vol. 1, no. 1, pp. 5–15, 2003.
- [24] M. Ouchi, S. Nakamura, T. Osterberg, S. Hallberg, and M. Lwin, "Applications of self-compacting concrete in Japan, Europe and the United States", *Kochi University of Technology, Kochi, Japan*, 2003.

- [25] M. Khrapko, "Self Compacting Concrete – a Solution for Technology Hungry Concrete Construction," Civil Engineering Testing Conference. pp. 1–9, 2008.
- [26] F. Junker, and K. Holschemacher, "Concrete-to-Concrete Bond of an Interface between Self-Consolidating Concrete and Vibrated Concrete", In: Khayat, K. H. (Hrsg.): SCC 2016 - 8th International RILEM Symposium on Self-Compacting Concrete. Washington, D.C., USA, 15-18 May 2016. RILEM proceedings PRO, Heft 100, S. 413–422. RILEM Publications S.A.R.L, Paris, France, 2016.
- [27] H.M. Albegmprli, M.E. Gülşan, and A. Cevik, "Comprehensive experimental investigation on mechanical behavior for types of reinforced concrete Haunched beam", *Advances in Concrete Construction*, vol. 7, no. 1, pp. 39, 2019.
- [28] S. Y. D. and E. I. Elniema, "Behavior and Strength of Reinforced Concrete Haunched Beams in Shear," *ACI J. Proc.*, vol. 79, no. 3, 1982.
- [29] I.A. Macleod, and A. A. Houmsi, "Shear Strength of Haunched Beams Without Shear Reinforcement", *ACI Structural Journal*, vol. 91, no. 1, pp. 79–89, 1991.
- [30] G. Stefanou, Shear resistance of reinforced concrete beams with non-prismatic sections. *Engineering Fracture Mechanics*, vol. 18, no. 3, pp. 643–666, 1983.
- [31] A. Tena-Colunga, H. I. Archundia-Aranda, and Ó. M. González-Cuevas, "Behavior of reinforced concrete haunched beams subjected to static shear loading," *Eng. Struct.*, vol. 30, no. 2, pp. 478–492, 2008.
- [32] V. H. Nghiep, "Shear design of straight and haunched concrete beams without stirrups," Doktor Thesis. 2011.
- [33] G. A. Rombach, M. Kohl, and V. H. Nghiep, "Shear design of concrete members without shear reinforcement - A solved problem?" *Procedia Engineering*, vol. 14. pp. 134–140, 2011.
- [34] C. HOU, K. MATSUMOTO, and J. NIWA, "Shear Failure Mechanism of Reinforced Concrete Haunched Beams," *Journal of JSCE*, vol. 3, no. 1. pp. 230–245, 2015.
- [35] T. Al-Attar, S. Abdulqader, and S. Ibrahim, "Behavior of Tapered Self-Compacting Reinforced Concrete Beams Strengthened by CFRP", *Engineering and Technology Journal*, vol. 35, no. 3 (Part (A) Engineering), 1982.pp. 197-203, 2017.
- [36] M.S. Al Jawahery, M.E. Gulsan, H.M. Albegmprli, I.A.H. Mansoori, and A. Cevik, "Experimental investigation of rehabilitated RC haunched beams via CFRP with 3D-FE modelling analysis", *Engineering Structures*, vol. 196, no. 109301, pp. 1-25, 2019.
- [37] M. Maalej and V. C. Li, "Flexural/Tensile-Strength Ratio in Engineered Cementitious Composites," *J. Mater. Civ. Eng.*, vol. 6, no. 4, pp. 513–528, 1994.
- [38] M. Maalej, and V.C. Li, "Introduction of strain-hardening engineered cementitious composites in design of reinforced concrete flexural members for improved durability", *ACI Structural Journal*, vol. 92, no. 2, pp. 167-176, 1995.
- [39] S. B. Singh and M. V. R. Sivasubramanian, "Performance of ductile fibre-reinforced cementitious composite concrete frames under flexural loading," *Proc. Inst. Civ. Eng. - Constr. Mater.*, vol. 166, no. 1, pp. 34–44, 2013.
- [40] J. ZHANG, C. LEUNG, and Y. CHEUNG, "Flexural performance of layered ECC-concrete composite beam," *Compos. Sci. Technol.*, vol. 66, no. 11–12, pp. 1501–1512, 2006.
- [41] F. Yuan, J. Pan, and Y. Wu, "Numerical study on flexural behaviors of steel reinforced engineered cementitious composite (ECC) and ECC/concrete composite beams," *Sci. China Technol. Sci.*, vol. 57, no. 3, pp. 637–645, 2014.
- [42] Y. Guan, H. Yuan, Z. Ge, Y. Huang, S. Li, and R. Sun, "Flexural properties of ECC-concrete composite beam," *Advances in Civil Engineering*, vol. 2018. 2018.
- [43] M. R. Islam, M. A. Mansur, and M. Maalej, "Shear strengthening of RC deep beams using externally bonded FRP systems," *Cement and Concrete Composites*, vol. 27, no. 3. pp. 413–420, 2005.
- [44] ASTM C39/C39M-12, Standard Test Method For Compressive Strength Of Cylindrical Concrete Specimens; Annual book of ASTM standard, (Vol. 4-2), Philadelphia, PA, USA, 2012.
- [45] BS, Testing Concrete: Method for determination of compressive strength of concrete cubes., British Standard Institution London, 1983.
- [46] A. K. Al-Asadi, "Application of external prestressing on the rehabilitation of reinforced concrete beams," *Periodicals of Engineering and Natural Sciences*, vol. 7, no. 3. pp. 974–984, 2019.

- [47] ASTM C 496/C 496M-11, Standard Test Method for Splitting Tensile Strength of Cylindrical Concrete, ASTM, West Conshohocken, PA, 5 , 2011.
- [48] ASTM C 469, Standard test method for static modulus of elasticity and Poisson's ratio of concrete in compression, Annual Book of ASTM standards, vol. 04.02, 2002.
- [49] Y. Zhu, Y. Yang, and Y. Yao, "Use of slag to improve mechanical properties of engineered cementitious composites (ECCs) with high volumes of fly ash," *Construction and Building Materials*, vol. 36. pp. 1076–1081, 2012.
- [50] BASF chemical company, "Product Technical Epoxy Resin for MasterBrace", 2018.
- [51] Du Béton, F.I., "Externally bonded FRP reinforcement for RC structures", *Bulletin*, 14, pp. 138, 2001.
- [52] 440, A.C.I.C. Guide for the Design and Construction of Externally Bonded FRP Systems for Strengthening Concrete Structures: ACI 440.2 R-08. American Concrete Institute, 2008.